Nontraumatic Spinal Cord Compression: MRI Primer for Emergency Department Radiologists

Olga Laur, MD, MHS
Hari Nandu, MD[1]
David S. Titelbaum, MD
Diego B. Nunez, MD, MPH
Bharti Khurana, MD

Abbreviations: ADEM = acute disseminated encephalomyelitis, AQP4-IgG = aquaporin-4 immunoglobulin G, CSF = cerebrospinal fluid, DAVF = dural arteriovenous fistula, MS = multiple sclerosis, NMO = neuromyelitis optica, STIR = short τ inversion-recovery

RadioGraphics 2019; 39:1862–1880

https://doi.org/10.1148/rg.2019190024

Content Codes: ER MR NR OI

From the Departments of Radiology (O.L., D.B.N.), Neuroradiology (H.N., D.B.N.), and Emergency Radiology (B.K.), Brigham and Women's Hospital, 75 Francis St, Boston, MA 02115; and Department of Radiology, Shields Health Care, Brockton, Mass (D.S.T.). Recipient of a Certificate of Merit award for an education exhibit at the 2018 RSNA Annual Meeting. Received February 15, 2019; revision requested April 29 and received June 28; accepted July 25. For this journal-based SA-CME activity, the author B.K. has provided disclosures (see end of article); all other authors, the editor, and the reviewers have disclosed no relevant relationships. **Address correspondence to** O.L. (e-mail: *olga.laur@bwh.harvard.edu*).

[1]Current address: CP Advanced Imaging, New York, NY.

SA-CME LEARNING OBJECTIVES

After completing this journal-based SA-CME activity, participants will be able to:

- Describe the anatomy of the spinal canal compartment and localize compressive lesions to an epidural, intradural extramedullary, or intramedullary space.
- Differentiate common compressive causes of acute myelopathy according to compartment location and characteristic imaging findings.
- List common causes of noncompressive myelopathy and refine the differential diagnosis according to the location and longitudinal extension of abnormal signal intensity within the spinal cord, neural tracts involved, and ancillary clinical history and laboratory data.

See rsna.org/learning-center-rg.

The occurrence of acute myelopathy in a nontrauma setting constitutes a medical emergency for which spinal MRI is frequently ordered as the first step in the patient's workup. The emergency department radiologist should be familiar with the common differential diagnoses of acute myelopathy and be able to differentiate compressive from noncompressive causes. The degree of spinal cord compression and presence of an intramedullary T2-hyperintense signal suggestive of an acute cord edema are critical findings for subsequent urgent care such as surgical decompression. Importantly, a delay in diagnosis may lead to permanent disability. In the spinal canal, compressive myelopathy can be localized to the epidural, intradural extramedullary, or intramedullary anatomic spaces. Effacement of the epidural fat and the lesion's relation to the thecal sac help to distinguish an epidural lesion from an intradural lesion. Noncompressive myelopathy manifests as an intramedullary T2-hyperintense signal without an underlying mass and has a wide range of vascular, metabolic, inflammatory, infectious, and demyelinating causes with seemingly overlapping imaging appearances. The differential diagnosis can be refined by considering the location of the abnormal signal intensity within the cord, the longitudinal extent of the disease, and the clinical history and laboratory findings. Use of a compartmental spinal MRI approach in patients with suspected nontraumatic spinal cord injury helps to localize the abnormality to an epidural, intradural extramedullary, or intramedullary space, and when combined with clinical and laboratory findings, aids in refining the diagnosis and determining the appropriate surgical or nonsurgical management.

Online supplemental material is available for this article.

Introduction

Acute compressive myelopathy in the setting of minimal to no trauma is a medical emergency for which timely intervention is essential to minimize irreversible loss of neurologic function. Decompression of the spinal cord within the first 24 hours after the onset of myelopathy has been shown to improve neurologic outcomes (1–3). As a result, MRI of the spine is frequently performed on an emergent basis, including after hours, to assess suspected cord compression. Thus, it is imperative that emergency department radiologists have a good understanding of the common differential diagnoses of acute myelopathy and be able to differentiate the compressive versus noncompressive causes. The anomalies commonly included in the differential diagnosis of acute myelopathy and the compressive and noncompressive causes of this disease are described in this review.

TEACHING POINTS

- An intramedullary T2-hyperintense signal of the spinal cord by itself is a nonspecific finding and cannot be used to reliably predict surgical outcomes. However, a high T2 signal intensity change when comparing a compressed segment to a noncompressed segment, or a low T1 signal intensity change with high T2 signal intensity of the compressed segment, has been associated with worse outcomes, as these differences may indicate advanced histologic damage.
- MRI reveals a T1-hypointense, T2-hyperintense epidural collection that may enhance diffusely in a phlegmon state or show peripheral enhancement, with central nonenhancement, in cases of a mature abscess. The collection is rarely an isolated finding and almost always is associated with spondylodiscitis and paravertebral muscle involvement.
- Neurofibromas, and to a lesser degree schwannomas, tend to have a characteristic "target sign" appearance, with central T2 hypointensity and peripheral T2 hyperintensity.
- It is important to note that in cases of slow flow during early DAVF, these venous plexi may not be well seen at T2-weighted MRI. In such cases, contrast-enhanced MRI is the most reliable modality for visualizing dilated serpentine enhancing perimedullary vessels, which are suggestive of DAVF.
- The classic triad of NMO consists of optic neuritis, longitudinally extensive transverse myelitis involving more than three vertebral segments, and serologic analysis findings positive for AQP4-IgG antibody.

"Red Flags" for Myelopathy and Importance of Spinal MRI in the Clinical Workup

Myelopathy is defined as a neurologic deficit secondary to a spinal cord abnormality. Classic "red flags" for myelopathy include rapidly developing muscle weakness, sensory deficit, and loss of bowel and bladder sphincter control (4). Cauda equina syndrome is a myelopathy characterized by saddle anesthesia, loss of bowel and bladder control, sexual dysfunction, and frequently lower extremity weakness (5). The clinical history and laboratory values indicative of infection or malignancy can further influence the decision to pursue MRI.

According to the American College of Radiology Appropriateness Criteria, patients who present with symptoms of nontraumatic painful or sudden-onset progressive myelopathy should undergo MRI of the spine without contrast material. In cases of suspected infection, concern for malignancy, or a suspected inflammatory or vascular cause, contrast material–enhanced spinal MRI is preferable. If vascular disease is suspected, spinal MR angiography can be performed as an adjunctive examination.

MRI can be used to directly determine compressive versus noncompressive causes of myelopathy, assess for intramedullary disease, and determine the specific spinal level of involvement. Sagittal and axial T1- and T2-weighted and short τ inversion-recovery (STIR) MRI sequences typically are used and may be supplemented by fat-suppressed, gradient-echo, diffusion-weighted, and contrast-enhanced sequences (Table).

Anatomic Compartment–based Approach to Myelopathy

Knowledge of the spinal canal anatomy is critical for localizing myelopathies, and acquiring an understanding of this anatomy should be the first step in the spinal MRI evaluation. Myelopathies can be broadly attributed to compressive or noncompressive causes. Compressive myelopathy results from a lesion's external compression on the spinal cord and can be further localized to an extradural, intradural extramedullary, or intramedullary space. It is important to understand that an intramedullary T2-hyperintense signal in the setting of symptoms of acute cord compression is an urgent finding and probably indicates acute cord edema and ischemia. Lesions associated with cord atrophy and chronic blood products probably represent irreversible changes such as necrosis and cavitation and may not respond to treatment.

Noncompressive myelopathy is confined to the intramedullary space and is not associated with an underlying space-occupying lesion. Whereas compressive myelopathy is commonly managed with neurosurgical decompression, treatment of noncompressive myelopathy depends on the specific cause of the disease.

Localization of Compressive Myelopathy

Epidural space is defined as the space between the bony spinal canal and the dura mater. It contains epidural fat, spinal nerves, small arterioles, venous plexi, and lymphatics and communicates directly with the paravertebral space by way of the intervertebral foramina. *Intradural space* is defined as the space between the arachnoid mater and pia mater. It contains cerebrospinal fluid (CSF), nerve fibers, vascular elements, and glial tissue. The potential subdural space lies between the arachnoid mater and dura mater, which are closely opposed to each other secondary to bridging thin strands of collagen (6). Finally, the intramedullary compartment is the space within the substance of the spinal cord.

On MR images, the dura mater and arachnoid mater are difficult to differentiate owing to their close proximity. They appear as a T1- and T2-hypointense membrane defining the thecal sac (Fig 1), with epidural space external to the thecal sac and intradural space internal to it. At MRI, a compressive lesion in the epidural space causes effacement of the epidural fat, inward displacement of the dura mater, and compression of the spinal cord (Fig 2, Table E1). T2-weighted MRI

Sequences That Can Be Added to the Spinal MRI Protocol for Myelopathy

MRI Sequence	Assessed Pathologic Entity
Contrast-enhanced T1 weighted	Metastatic, infectious, inflammatory, or autoimmune disease
Contrast-enhanced fat-saturated T1 weighted	Lipomatous epidural lesions vs nonlipomatous phlegmon or metastasis
Gradient echo	Epidural hematoma, intramedullary cavernous malformation
Diffusion weighted	Spinal cord infarction, abscess

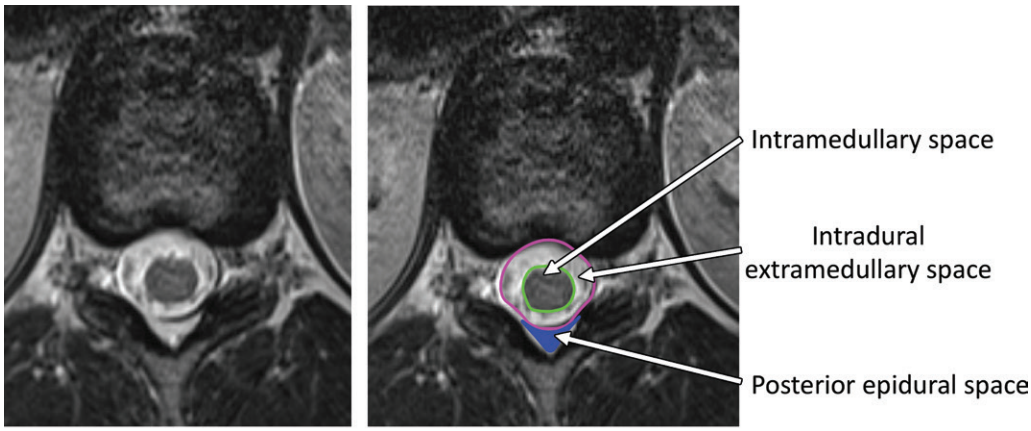

Figure 1. MRI findings in a healthy 23-year-old woman. Axial nonlabeled **(a)** and labeled **(b)** T2-weighted MR images of the thoracic spine at the T11-T12 spinal level show the thecal sac (pink outline in **b**) and pia mater (green outline in **b**), which compartmentalize the spinal canal into the epidural, intradural extramedullary, and intramedullary spaces. In **b**, the posterior epidural space (blue) is filled with fat.

has been shown to have the highest inter- and intrareader reliability for grading the degree of compression, with *high-grade compression* defined as deformation of the spinal cord with partial or complete obliteration of the CSF space (7).

In contrast, an intradural lesion is located deep to the thecal sac, with preservation of the epidural fat, on MR images (Table E2). Because lesions in the intradural space lie within the CSF, there is usually ipsilateral enlargement of the CSF space to accommodate the space-occupying lesion. A cleft of CSF may be seen separating the lesion from the spinal cord. Finally, an intramedullary lesion results in expansion of the spinal cord.

Noncompressive Myelopathy

At MRI, noncompressive myelopathy manifests as an abnormal T2-hyperintense signal within the spinal cord. It has a wide range of vascular, metabolic, inflammatory, infectious, and demyelinating causes with seemingly overlapping imaging appearances (Table E3). The differential diagnosis can be refined by considering the lesion's location within the cord, its longitudinal extent, and the pertinent clinical history and laboratory findings.

Epidural Causes of Compressive Myelopathy

Degenerative Disease

Disk Herniation.—Spondylotic myelopathy secondary to acute disk herniation is the most common cause of cauda equina syndrome and the most common cause of spinal cord dysfunction in adults worldwide (5,8). Disk extension into the anterior epidural space varies from a broad disk bulge to a focal herniation. The herniation can be further categorized as disk protrusion, extrusion, or sequestration (9). Acute neurologic deficit due to acute disk extrusion is a potential neurosurgical emergency. More chronic forms of disk extrusion can be addressed with cord adaptation and may be asymptomatic. In many cases, the degree of disk herniation can regress with time (10).

At MRI, the epidural component of the herniated disk has the same signal intensity characteristics as the donor disk (Fig 3). In cases of seques-

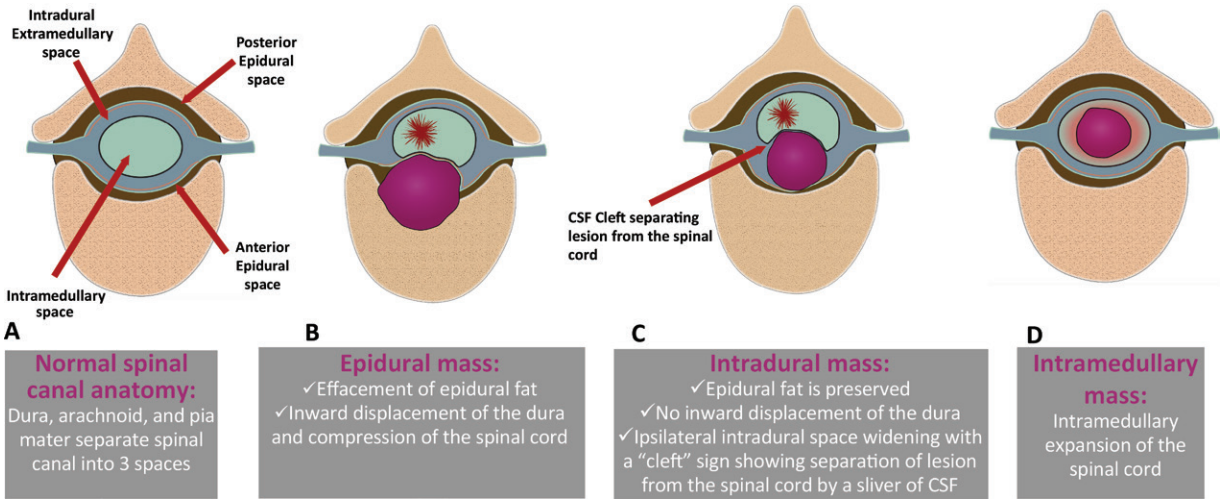

Figure 2. Drawings illustrate the anatomic compartments of the spinal canal and their typical imaging appearances in the presence of a space-occupying lesion. The normal axial anatomy of the spinal cord *(A)* and the axial appearances of the spinal cord when a mass is localized to the epidural *(B),* intradural extramedullary *(C),* and intramedullary *(D)* spaces are depicted.

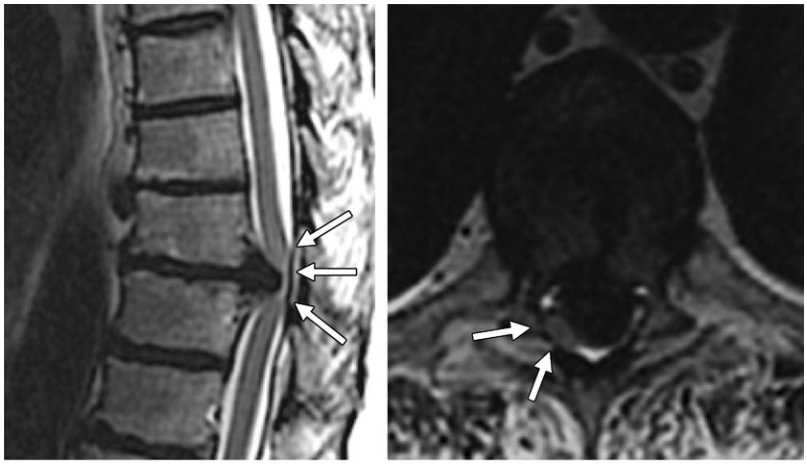

Figure 3. Acute disk herniation in a 50-year-old man who presented with leg numbness and weakness. Sagittal **(a)** and axial **(b)** T2-weighted MR images of the thoracic spine show intervertebral disk extrusion at the T11-T12 spinal level, with posterolateral displacement and significant compression on the spinal cord (arrows in **b**). Note the continuity of the extruded disk with the donor disk. The focal increase in spinal cord signal intensity (arrows in **a**) probably indicates acute cord edema.

tration, owing to its increased fluid component, the fragment may appear to have higher signal intensity than the donor disk at T2-weighted MR imaging. Frequently, a layer of granulation tissue surrounds the avascular sequestered material, causing it to have peripheral enhancement (11).

Spinal Canal Stenosis.—Acquired spinal canal stenosis represents multifactorial degenerative changes characterized by facet joint hypertrophy, disk bulging or herniation, multilevel endplate osteophytes, buckling of the ligamentum flavum, and ligamental ossification. In addition, nerve root and spinal cord compression can be aggravated by dynamic mechanisms, particularly in the cervical spine. MR images show an hourglass appearance of the spinal canal, with effacement of the CSF space (Fig 4). If the lumbar region is affected, the cauda equina nerve roots may have a crowded, serpiginous appearance (12,13).

An intramedullary T2-hyperintense signal of the spinal cord by itself is a nonspecific finding and cannot be used to reliably predict surgical outcomes. However, a high T2 signal intensity change when comparing a compressed segment to a noncompressed segment, or a low T1 signal intensity change with high T2 signal intensity of the compressed segment has been associated with worse outcomes, as these differences may indicate advanced histologic damage (8). Chronic mechanical compression of the spinal cord can lead to cord flattening and enhancement, with destruction of the blood–spinal cord barrier.

Infectious Disease

Epidural abscess is usually secondary to spondylodiscitis and less commonly secondary to septic arthritis. The abscess typically extends into the anterior or posterior epidural space and may

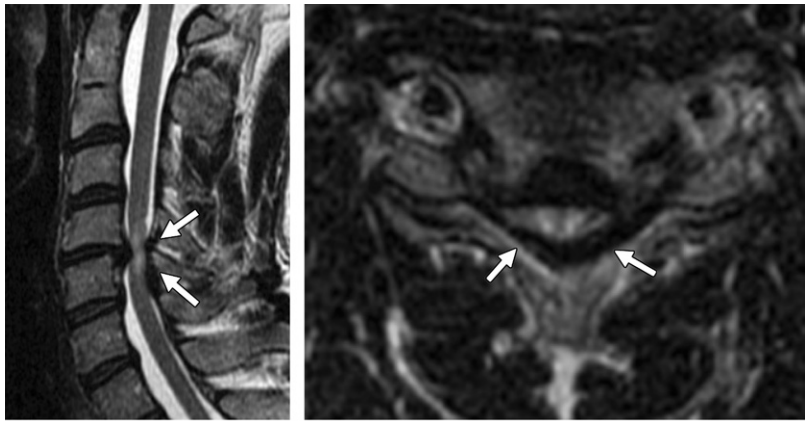

Figure 4. Spinal stenosis and cord compression in a 48-year-old man who had progressive gait disturbance of several months duration and bowel and bladder dysfunction for 2 days. Sagittal **(a)** and axial **(b)** T2-weighted MR images of the cervical spine show severe cervical stenosis at the C4-C5 spinal level secondary to a herniated disk–osteophyte complex extending into the anterior epidural space, and buckling of the ligamentum flavum in the posterior epidural space (arrows). These findings result in complete focal CSF effacement and ventral and dorsal cord compression with intramedullary T2 hyperintensity.

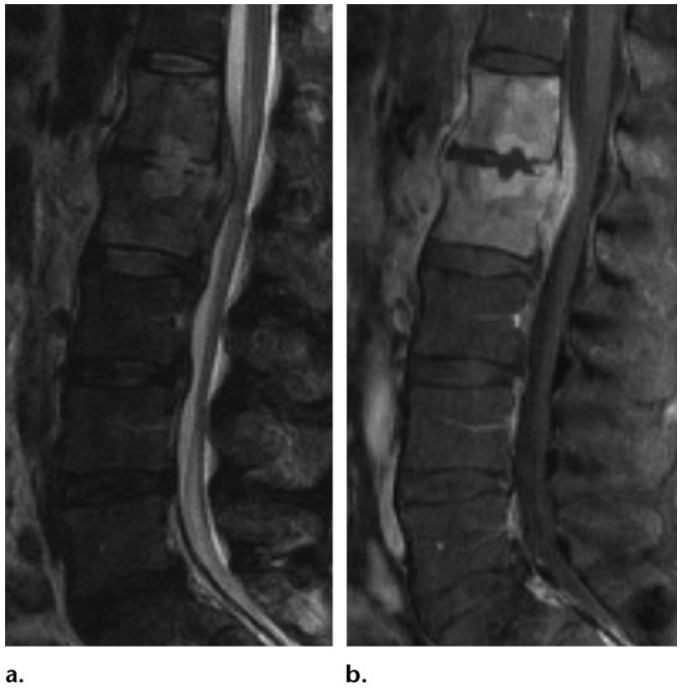

Figure 5. L1–L2 spondylodiscitis with an epidural phlegmon in a 50-year-old man who presented with bilateral lower extremity weakness. **(a, b)** Sagittal T2-weighted **(a)** and contrast-enhanced T1-weighted **(b)** MR images of the lumbar spine show T2-hyperintense, abnormally enhancing L1-L2 vertebral bodies, with intervertebral disk destruction and an anterior epidural homogeneously enhancing phlegmon spanning the L1-L2 vertebra. **(c)** Axial contrast-enhanced T1-weighted MR image of the lumbar spine at the L1-L2 level shows posterior displacement of the thecal sac by the phlegmon (arrows). There is also diffuse prevertebral and paraspinal enhancement (arrowheads), indicating an intramuscular phlegmon.

result in myelopathy secondary to either mass effect on the thecal sac or septic thrombophlebitis. Symptoms can progress from pain and radiculopathy to weakness and eventual paralysis. An epidural abscess is a surgical emergency for which appropriate management is critical to preventing paralysis.

Neurologic deficit is the most important factor in the treatment decision of surgical débridement versus medical therapy only (14). Spinal instability in the setting of spondylodiscitis with bone destruction, severe deformity, and/or kyphosis also contributes to the cord compression and symptoms of myelopathy and is a frequent indication for surgical management (15). *Staphylococcus aureus* is the most common pathogen. Intravenous drug use and immunosuppression are predisposing factors for spinal epidural abscess formation.

MRI reveals a T1-hypointense, T2-hyperintense epidural collection that may enhance diffusely in a phlegmon state or show peripheral enhancement, with central nonenhancement, in cases of a mature abscess (Figs 5, 6). The collection is rarely an isolated finding and almost

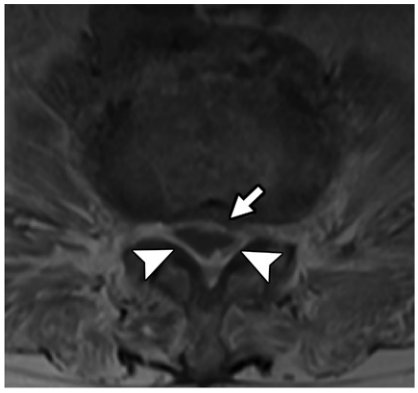

a.

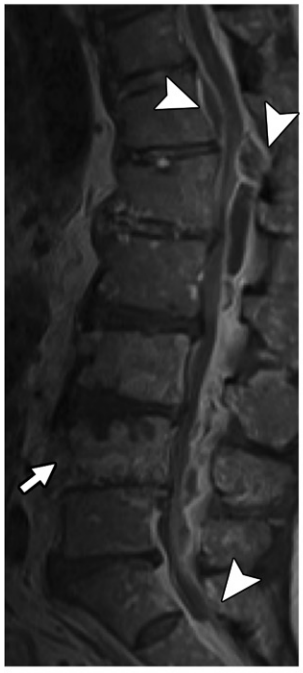

b.

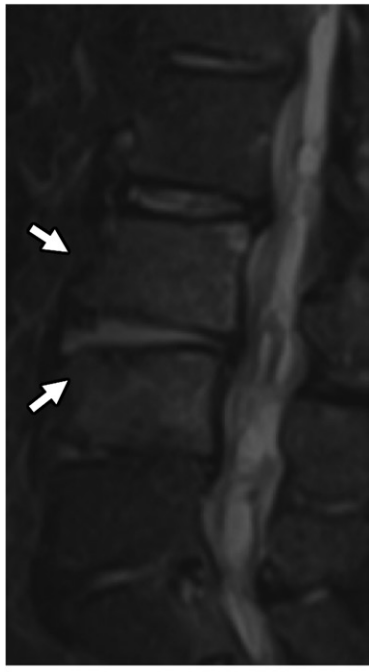

c.

Figure 6. L3-L4 spondylodiscitis and a large epidural abscess, with blood cultures yielding methicillin-sensitive *S aureus,* in a 65-year-old man. Axial contrast-enhanced T1-weighted MR image at the L1-L2 level **(a)** and sagittal contrast-enhanced T1-weighted **(b)** and STIR **(c)** MR images of the lumbar spine show an elongated T2-hyperintense peripherally enhancing collection with an anterior epidural component at the T12 level, extensive posterior epidural extension to the S1 level (arrowheads in **a** and **b**), and anterior thecal sac displacement and compression at the L1-L2 level (arrow in **a**). L3-L4 spondylodiscitis is also depicted; it is seen as abnormal hyperintensity of the intervertebral disk and adjacent bone at STIR imaging and as abnormal bone enhancement at contrast-enhanced imaging (arrows in **b** and **c**).

always is associated with spondylodiscitis and paravertebral muscle involvement (16).

Vascular Disease

Atraumatic development of an epidural hematoma can be seen in the setting of anticoagulation therapy or coagulopathy, vascular malformations, Paget disease, and/or iatrogenic causes. In the setting of rapidly progressive symptoms, an epidural hematoma is considered a surgical emergency, as a delay in decompression may result in permanent deficits. Epidural hematomas occur most commonly in the cervical or thoracic spine, typically in the dorsal epidural space. The classic appearance is characterized by a biconvex morphology (Fig 7). An epidural hematoma has variable signal intensity at T1- and T2-weighted MRI, depending on the age of the blood products, which has been described in the literature (17).

It should be noted that a hyperacute hematoma that has existed for less than 24 hours is expected to appear T1 isointense and T2 hyperintense and thus is difficult to distinguish from CSF. Displacement of the thecal sac and effacement of the epidural fat are subtle clues to the underlying space-occupying lesion. Epidural hematoma typically has peripheral enhancement on contrast-enhanced images. The presence of enhancing foci may indicate active extravasation.

Metastatic Disease

The spine is the most common site of skeletal metastases, with an annual prevalence of malignant spinal cord compression of approximately 3%–5%. Metastatic spinal disease represents the initial manifestation of malignancy in approximately 20% of patients (18,19). Involvement of the spinal column with epidural cord compression is significantly more common than intradural and

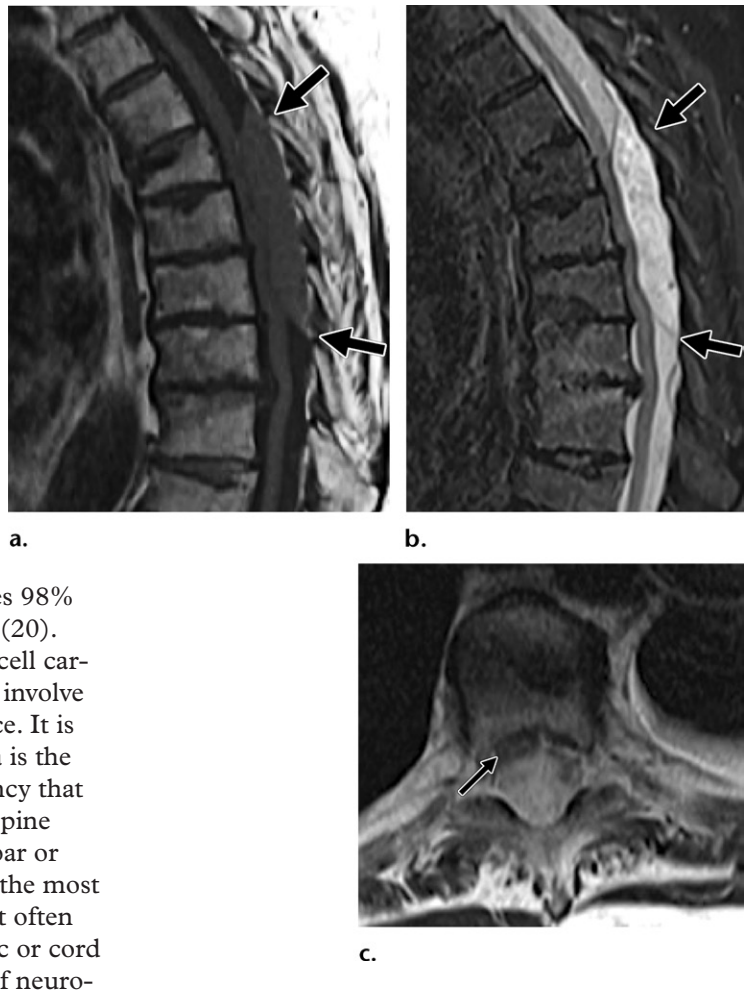

Figure 7. Epidural hematoma in an 84-year-old woman after a fall and epidural catheter placement for pain, with rapid development of lower extremity weakness. **(a, b)** Sagittal T1-weighted **(a)** and STIR **(b)** MR images of the thoracic spine show a large biconvex heterogeneous collection (arrows) in the posterior epidural space, extending from the T6 to T9 vertebral level. The collection is T1 isointense and has high signal intensity at STIR MRI. **(c)** Axial T2-weighted image at the T8 level shows effacement of the posterior epidural fat and ventral displacement of the spinal cord, with severe compression (arrow).

intramedullary metastases and constitutes 98% of cases of spinal cord metastatic lesions (20). Prostate, lung, and breast cancers; renal cell carcinoma; and lymphoma most commonly involve the spine and extend to the epidural space. It is important to note that multiple myeloma is the most common primary osseous malignancy that can lead to cord compression. Thoracic spine compression is more common than lumbar or cervical spine compression. Back pain is the most common symptom at presentation, and it often worsens at night. The degree of thecal sac or cord compression correlates with the degree of neurologic impairment and the functional outcome.

Hematogenous spread is most common, with vertebral body involvement being more common than posterior element involvement, presumably because of the high vascularity and larger volume of the vertebral body. Cord compression results from the spread of metastasis from the vertebral body to the dura, direct infiltration of the dura, and transforaminal extension. Even in the absence of significant mass effect, a hyperintense signal may be seen in the spinal cord at T2-weighted MRI. This high signal intensity is suggestive of edema that may be caused by a vascular phenomenon such as venous hypertension secondary to impingement of the epidural venous plexi by the tumor.

MRI aids in assessing the presence and extent of osseous involvement, paravertebral and epidural extension, and thecal sac impingement. Since metastatic disease commonly occurs at multiple levels and recurrent disease is common, contrast-enhanced MRI of the entire spine is performed (21). An epidural tumor typically is hypointense at T1-weighted MRI, has variable signal intensity at T2-weighted MRI, and has variable enhancement depending on the degree of necrosis and/or sclerosis (Figs 8, 9).

The degree of epidural cord compression can be graded—for example, by using the Epidural Spinal Cord Compression Scale—to help determine whether the patient may benefit from radiation treatment or surgical decompression. In addition, various models, such as the Spinal Instability Neoplastic Score (SINS) model, have been developed to aid in interpreting images and triaging cases of spine instability in patients with oncologic conditions. In such models, a high score indicates the need for urgent surgical intervention. Factors such as location of the metastatic lesion, alignment of the spine, degree of vertebral body involvement, lesion appearance, and degree of pain are considered in the SINS model (22).

Metabolic Disease

Extramedullary hematopoiesis expansion outside the bone marrow occurs in the setting of ineffective erythropoiesis. It is associated with myelofibrosis, sickle cell anemia, β thalassemia, lymphoma and leukemia, Gaucher disease, Paget disease, and pernicious anemia. Epidural extramedullary hematopoiesis is believed to result from hematopoietic rest cells in the spinal canal

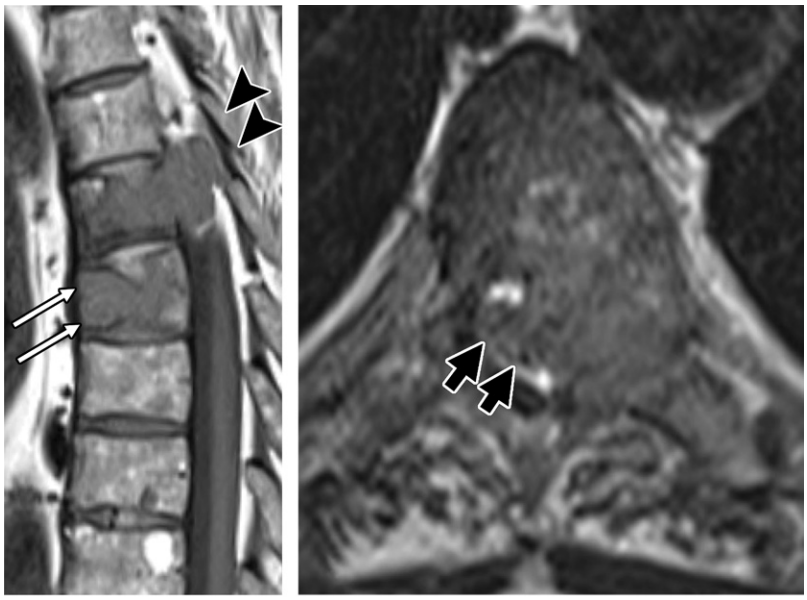

Figure 8. Metastatic prostate cancer in a 72-year-old man. Sagittal T1-weighted image of the thoracic spine **(a)** and axial T2-weighted image at the T7 vertebral level **(b)** show a destructive soft-tissue mass involving the T7 vertebral body and left posterior elements, with extension into the anterior epidural space (arrowheads in **a**) and lateral displacement and compression of the spinal cord (arrows in **b**). An additional T1-hypointense lesion (arrows in **a**) in the T8 vertebra is noted.

Figure 9. Lymphoma in a 55-year-old man. Sagittal T2-weighted **(a)** and contrast-enhanced T1-weighted **(b)** MR images of the lumbar spine show multiple enhancing masses in the anterior and posterior epidural space. **(c)** Axial T2-weighted image at the L4 vertebral level shows effacement of the posterior epidural space, with anterior displacement of the thecal sac (arrows).

or direct extension of the paravertebral hematopoietic tissue into the spinal canal (23). It occurs most commonly in the middle to lower thoracic spine.

At MRI, well-defined multilevel epidural lobulated masses that are T1 hypointense and mildly T2 hyperintense are seen, often in association with extrapleural paravertebral masses. In extramedullary hematopoiesis, a T2-hypointense signal also may be seen and is secondary to the increased iron content in the hematopoietic tissue (Fig 10). Because active lesions are vascular, they enhance at contrast-enhanced imaging. Inactive older lesions often have more fat tissue and iron deposits.

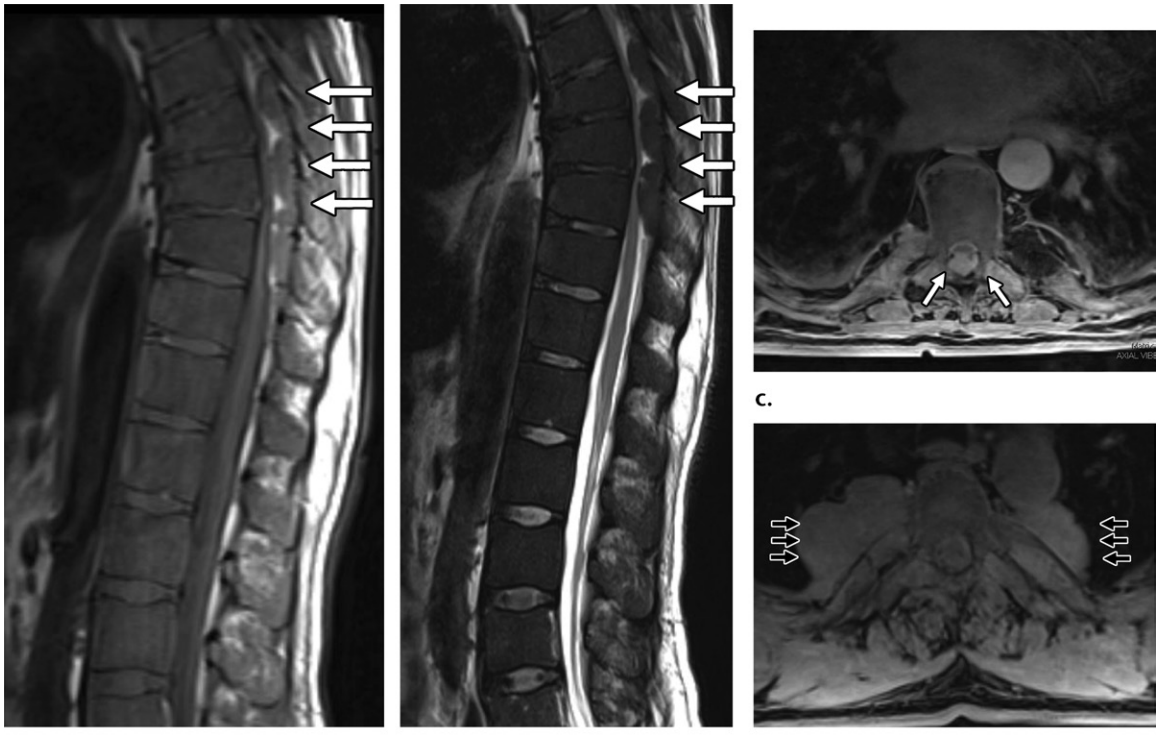

Figure 10. Extramedullary hematopoiesis in a 53-year-old man with a history of β thalassemia, who presented with lower-extremity weakness. Sagittal T1-weighted **(a)** and T2-weighted **(b)** MR images of the thoracolumbar spine, and axial contrast-enhanced T1-weighted MR images at the level of the abnormality **(c, d)** show multilevel lobulated T1-isointense and T2-hypointense avidly enhancing soft-tissue masses (arrows in **a** and **b**) in the posterior epidural space and associated large bilateral paravertebral extrapleural masses (arrows in **d**). These findings are typical of extramedullary hematopoiesis. There is also posterior epidural fat effacement and anterior displacement and deformation of the spinal cord (arrows in **c**). The diffuse decrease in T1 and T2 bone marrow signal intensity indicates red marrow conversion.

Other Epidural Causes of Compressive Myelopathy

Spontaneous cord herniation involves the thoracic spinal cord. The cord gradually herniates through the anterior or lateral defect in the dura to result in slowly progressive myelopathy. It affects patients in their 5th decade of life, has a female predominance, and is hypothesized to have a congenital cause (24). MR images show an abnormal contour of the spinal cord, with anterior kinking and an increase in dorsal CSF space. Cord deformation and narrowing may be present, with increased intramedullary T2 signal intensity. CSF turbulence artifact at the level of the herniation can help to differentiate a cord herniation from an intradural arachnoid cyst (Fig 11).

Intradural Causes of Compressive Myelopathy

Arachnoid Cyst

Arachnoid cyst represents a splitting of the arachnoid layer, which creates a potential space where CSF can accumulate. Patients commonly present with symptoms that indicate a slowly progressive myelopathy, which typically arises in the thoracic spine dorsal to the spinal cord. An arachnoid cyst has the signal intensity of CSF, with its walls often invisible on images and spinal cord displacement often being the only clue (25). The appearance of an arachnoid cyst often mimics that of thoracic cord herniation. Contrary to the thoracic cord herniation, space-occupying arachnoid cyst will displace the cord anteriorly, and, thus, CSF pulsation artifact will be absent. (Fig 12). Primary arachnoid cysts are congenital, while acquired arachnoid cysts can be caused by prior spinal surgery or lumbar puncture, trauma, or arachnoiditis.

Infection

An intradural extramedullary abscess is extremely rare and portends a poor prognosis (26). Few cases have been reported in the literature, and most of them have involved *S aureus* or *Mycobacterium tuberculosis* infections (27). Similar to the population at risk for epidural abscess, the population at risk for intradural extramedullary abscess includes immunocompromised patients, intravenous drug users, and patients who have recently undergone surgery. On MR images, an intradural abscess appears as an elongated T2-hyperintense,

a. b.

Figure 11. Thoracic cord herniation in a 65-year-old man. **(a)** Sagittal T2-weighted MR image of the thoracic spine shows a dorsal contour abnormality of the mid-thoracic spinal cord, with anterior cord deviation (white arrows) and expansion of the posterior CSF containing a prominent pulsation artifact (black arrows). **(b)** Axial T2-weighted MR image at the level of the abnormality shows focal anterior herniation of the spinal cord (arrows).

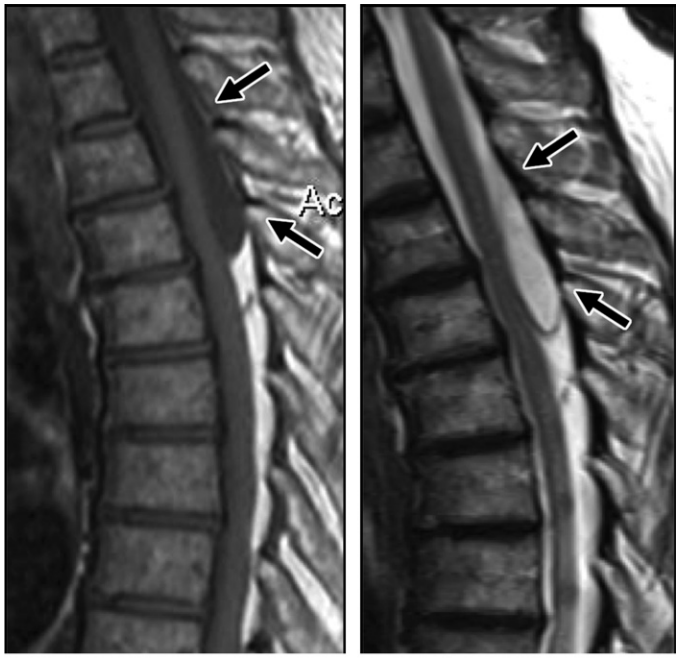

a. b.

Figure 12. Thoracic arachnoid cyst *(Ac)* in a 55-year-old woman. Sagittal T1-weighted **(a)** and STIR **(b)** MR images of the thoracic spine show a well-circumscribed ovoid cystic structure (arrows) in the posterior intradural space. The cyst has CSF signal intensity with all MRI sequences and exerts anterior mass effect on the spinal cord. The absence of CSF pulsation artifact posterior to the spinal cord abnormality should raise suspicion for an arachnoid cyst, even when the walls of the abnormality are not well seen.

T1-hypointense collection with peripheral enhancement. When the abscess is small, a phlegmon may mimic an intradural primary tumor such as schwannoma or meningioma.

Primary Tumors and Metastases

Meningioma.—The majority of intradural extramedullary tumors are meningiomas, schwannomas, or neurofibromas. A meningioma is usually a solitary mass, with the peak incidence occurring in individuals who are in their 5th–6th decade of life. Meningiomas typically are located anterior to the spinal cord in the cervical spine and posterior to the cord in the thoracic spine. A unique feature of meningioma is its broad dural base, with thickening and enhancement at contrast-enhanced MRI (28). This tumor may have intratumoral calcifications and prominent flow voids and rarely has a cystic appearance. On MR images, it appears as a T1- and T2-isointense avidly enhancing oval or round lesion (Fig 13). Multiple meningiomas are associated with neurofibromatosis type 2.

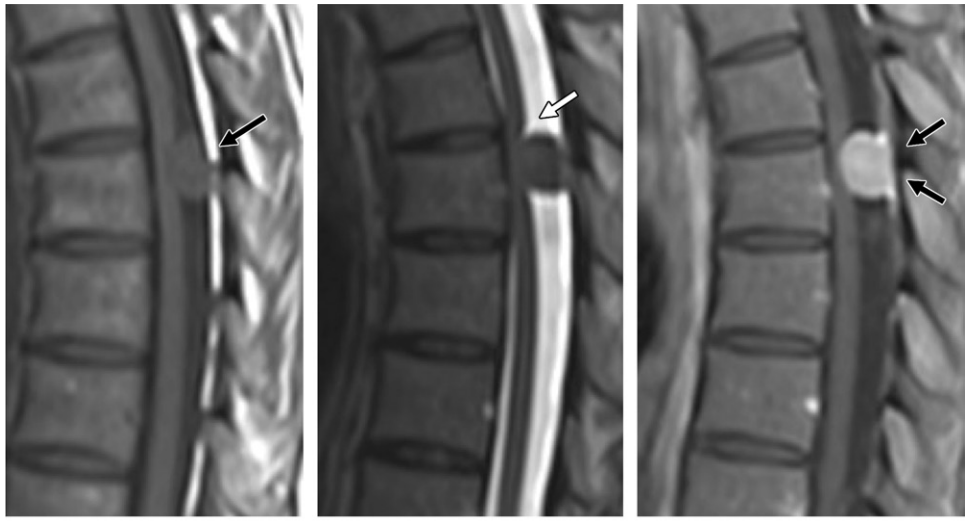

a. b. c.

Figure 13. Meningioma in a 46-year-old woman who presented with back pain, leg paresthesia, and difficulty urinating. Sagittal T1-weighted **(a)**, T2-weighted **(b)**, and contrast-enhanced fat-suppressed T1-weighted **(c)** MR images of the thoracic spine show a well-circumscribed oval posterior intradural T1- and T2-isointense mass with avid enhancement, broad dural attachment (arrows in **c**), and dorsal spinal cord compression. A cleft of CSF (arrow in **b**) is present between the mass and spinal cord, and the posterior epidural fat (arrow in **a**) is preserved, indicating an intradural location of the meningioma.

Schwannoma and Neurofibroma.—Schwannoma and neurofibroma are benign nerve sheath tumors that can be difficult to differentiate on MR images. The majority of these tumors are intradural, and approximately 15% of them have both intradural and extradural components. In those cases, a characteristic dumbbell-shaped lesion extends into and causes enlargement of the neural foramen (Fig 14). A schwannoma is an encapsulated neoplasm that can be removed during surgery when it is freed from the capsule, whereas a neurofibroma is intrinsically intertwined with the nerve and needs to be resected. Solitary schwannomas and neurofibromas tend to occur in individuals before their 6th decade of life. Multiple neurofibromas are common in patients with neurofibromatosis type 1 and have an earlier manifestation, while multiple schwannomas are common in patients with neurofibromatosis type 2 (29). Both of these lesions usually are T1 hypointense, with variable enhancement.

Neurofibromas, and to a lesser degree schwannomas, tend to have a characteristic "target sign" appearance, with central T2 hypointensity and peripheral T2 hyperintensity. Schwannomas tend to appear more heterogeneous on T2-weighted and contrast-enhanced MR images, secondary to cyst formation and vascular changes. Transformation to a malignant peripheral nerve sheath tumor should be suspected in cases of rapid growth, which is metabolically active at PET.

Intradural Metastases.—Intradural extramedullary spinal "drop" metastases represent hematogenous spread and frequently occur at the site of the conus medullaris. Lung, breast, and hematologic malignancies are common. The lumbar spine is the most frequently involved, and multifocal disease is common, with at least 50% of patients having brain metastases. Common symptoms include localized or radicular back pain, weakness, bladder dysfunction, and bowel dysfunction. On MR images, intradural metastases are deep to the dura, are typically T1 hypointense and T2 hyperintense, and enhance on contrast-enhanced images (Fig 15).

Vascular Disease

Intradural hematomas occur less frequently than do epidural hematomas and are more likely to be associated with coagulopathy and recent surgery than with trauma. Symptoms of acute myelopathy associated with intradural hematoma can occur more rapidly than those associated with epidural hematoma. On MR images, intradural hematomas are deep to the dura, with preservation of the epidural fat, and have T1 and T2 signal intensity that varies according to the age of blood products.

The morphology of an intradural hematoma may resemble an inverted Mercedes Benz sign, whereby the intradural collection is separated into two posterolateral components and one anterior component owing to the presence of intradural bilateral dentate ligaments and a dorsal midsagittal septum (17).

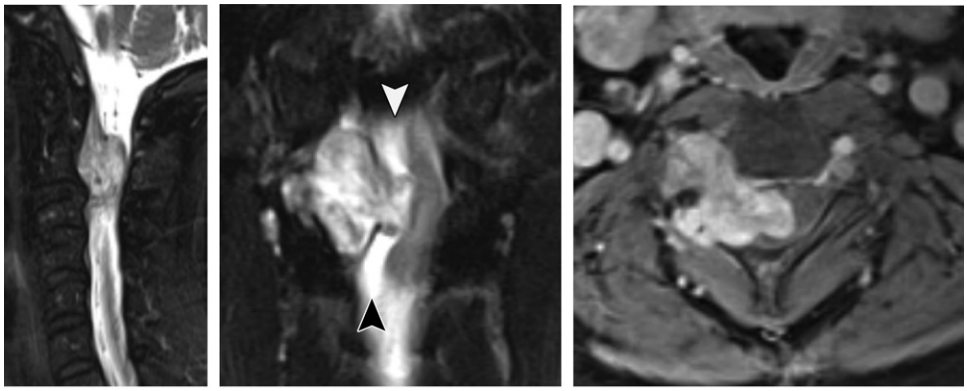

a. b. c.

Figure 14. Schwannoma with intradural and epidural components in a 65-year-old woman who presented with upper extremity weakness. Sagittal **(a)** and coronal **(b)** T2-weighted MR images of the cervical spine and axial contrast-enhanced T1-weighted MR image at the C2 spinal level **(c)** show a dumbbell-shaped T2-heterogeneous lesion with avid enhancement causing lateral displacement and compression of the spinal cord. The CSF cleft between the lesion and spinal cord is indicative of the intradural component (arrowheads in **b**) of the tumor.

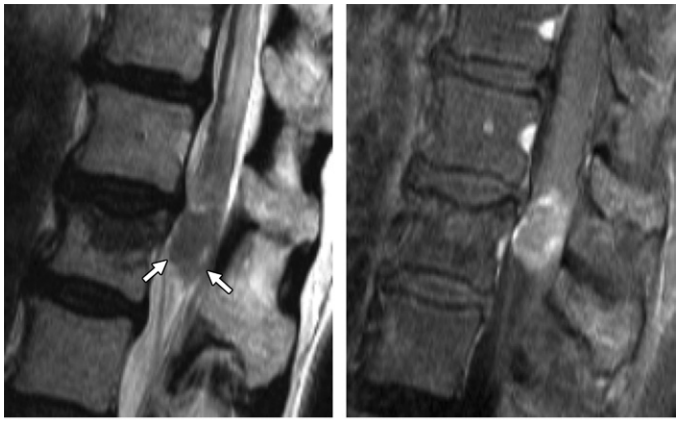

a. b.

Figure 15. Metastatic breast cancer in a 51-year-old woman who presented with new-onset bilateral leg weakness. Sagittal T2-weighted **(a)** and contrast-enhanced T1-weighted **(b)** MR images of the thoracolumbar spine show a large T2-hypointense enhancing intradural drop metastasis (arrows in **a**) at the level of the conus medullaris–cauda equina junction, with displacement of the cauda equina nerve roots and preservation of the posterior epidural fat. These findings are indicative of the intradural location of the metastasis. Leptomeningeal metastatic disease was identified at brain MRI (not shown).

Intramedullary Causes of Compressive Myelopathy

Intramedullary masses result in spinal cord expansion, and although different types of masses may be similar in appearance to each other, a few characteristic signs can help to narrow the differential diagnosis.

Intramedullary metastases represent a small percentage of the intramedullary tumor types and usually have edema that is out of proportion to the size of the lesion (Fig 16). Primary tumors include ependymoma, which is the most frequent adult intramedullary tumor; astrocytoma; and hemangioblastoma.

Ependymoma arises from glial cells that line the central canal and typically has an expansile well-circumscribed appearance, usually in the cervical cord (Fig 17). This tumor is slow growing, well defined, T2 hyperintense, and T1 hypointense, and it demonstrates avid enhancement (Fig 18). Polar cysts are commonly seen, and intratumoral cysts are less commonly seen (13). A T1-hyperintense signal may indicate intratumoral hemorrhage. The "tumor cap" sign is characteristic of ependymoma and appears as a T2-hypointense signal at the margin of the lesion secondary to the hemorrhage.

Astrocytoma is the second most common intramedullary tumor in adults and typically manifests within the cervical or thoracic spinal cord. Unlike ependymoma, astrocytoma is characterized by diffuse fusiform expansion of the cord, with the lesion not as sharply delineated. It is usually T2 hyperintense and T1 iso- to hypointense and has variable enhancement. An astrocytoma may have an eccentric growth pattern. Blood products are not as common with astrocytomas as they are with ependymomas.

Noncompressive Causes of Acute Myelopathy

Metabolic Cause

Subacute combined degeneration is a metabolic condition caused by vitamin B_{12} deficiency. It

a. b.

Figure 16. Intramedullary lung metastasis in a 46-year-old man. Sagittal STIR **(a)** and contrast-enhanced T1-weighted **(b)** MR images of the cervical spine show an enhancing intramedullary mass with peritumoral edema that is extensive and out of proportion to the size of the lesion.

results in a dorsal cord syndrome that is secondary to demyelination of the posterior columns. In severe cases, it also involves the corticospinal tracts. Subacute combined degeneration usually is secondary to B_{12} malabsorption and can be seen in patients who have pernicious anemia, have undergone bariatric surgery, or are on a strictly vegan diet. The onset of symptoms usually is insidious. Patients often present with sensory ataxia, paresthesia, and/or a history of frequent falls. They may also have spasticity and hyperreflexia with corticospinal tract involvement. Symptoms of dementia may be present in severe cases.

The abnormal signal intensity is usually contiguous in length, spanning several vertebral segments. At MRI, increased symmetric signal intensity on T2-weighted images, with corresponding hypointensity on T1-weighted images, is seen in the posterior columns, often with an inverted "V" configuration (Fig 19) (13). Mild enhancement caused by the breakdown of the blood–spinal cord barrier secondary to demyelination may be present. Treatment with parenteral B_{12} usually resolves symptoms, with the success of the treatment being dependent on the duration of the deficiency. Imaging abnormalities may not be completely resolved after treatment.

a. b.

Figure 17. Cervical spine ependymoma in a 51-year-old woman. Sagittal T2-weighted **(a)** and contrast-enhanced T1-weighted **(b)** MR images of the cervical spine show a well-defined expansile T2-heterogeneous intramedullary mass with avid contrast enhancement and large cranial and caudal polar cysts (arrows in **a**).

a. b.

Figure 18. Ependymoma in a 40-year-old woman. Sagittal STIR **(a)** and contrast-enhanced T1-weighted **(b)** MR images of the cervical spine show a central expansile intramedullary T2-hyperintense mass with a small amount of peritumoral edema and avid enhancement.

Vascular Causes

Spinal Cord Infarction.—Anterior spinal artery ischemia and spinal cord infarction cause ventral cord syndrome with involvement of the anterior

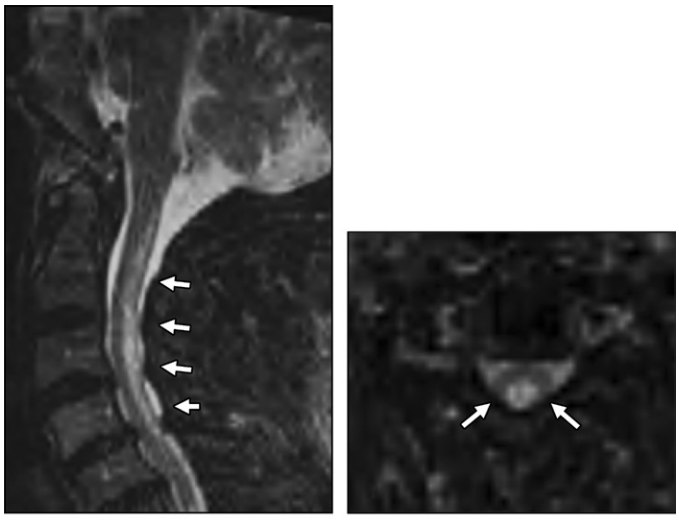

a. b.

Figure 19. Subacute combined degeneration in a 67-year-old man who presented with distal paresthesia, loss of proprioception, and a history of frequent falls. Sagittal STIR **(a)** and axial T2-weighted **(b)** MR images of the cervical spine show a multisegmental intramedullary T2-hyperintense signal abnormality (arrows) that is localized to the posterior columns and has an inverted "V" morphology.

two-thirds of the spinal cord. Patients present with acute and often painful symptoms of motor deficiency at the level below the level of infarction. These symptoms are often accompanied by bladder and/or bowel incontinence and spinothalamic tract involvement characterized by loss of temperature and pain sensation (13,30). Infarction of the posterior one-third of the spinal cord is rare secondary to the presence of bilateral posterior spinal arteries, as well as collateral vessels from the vascular pial plexus. In approximately half of patients, the cause of the infarction is unknown. Known causes include systemic hypotension secondary to shock, aortic or vertebral artery dissection, fibrocartilaginous emboli, a vascular complication after aortic surgery or coronary artery bypass graft placement, sickle cell disease, and/or cocaine abuse. Cord ischemia with venous hypertension also may occur in the setting of spinal arteriovenous malformation or epidural venous plexus thrombosis caused by an epidural phlegmon or tumor.

If cord ischemia is suspected, axial and sagittal diffusion-weighted imaging should be included in the MRI examination, as restricted diffusion is indicative of acute infarction. The transition from a normal appearance of the spinal cord to an abnormal appearance is typically well defined and indicative of an abnormality in the vascular territory. T2-weighted MRI reveals a linear pencil-like hyperintense signal within the spinal cord, corresponding to the ischemic vascular territory. Involvement of the anterior gray matter may cause an "owl's eye" appearance with corresponding high signal intensity at T2-weighted imaging (31). Of note, the intramedullary T2 signal intensity can appear normal during the first few hours after the onset of ischemia because the abnormal T2 signal intensity is proportional to the net inflow of edema (32).

T1-weighted MRI reveals spinal cord expansion in the acute phase. In rare cases of hemorrhagic conversion, the spinal cord will appear T1 hyperintense. Diffusion-weighted images show corresponding restricted diffusion secondary to cytotoxic edema (Fig 20). The restricted diffusion should resolve within a week, but the T2-hyperintense signal abnormality will persist. There may be an associated signal intensity abnormality of the adjacent vertebral bodies corresponding to bone marrow infarction.

Dural Arteriovenous Fistula.—Dural arteriovenous fistula (DAVF) of the spinal cord most commonly affects elderly men with symptoms of progressive myelopathy. These symptoms include gait disturbance, paresthesia, sensory loss, and radicular pain, which can be aggravated by exercise and eventually progress to bowel and bladder dysfunction. DAVF is one of the most common vascular lesions of the spine. It is considered to be an acquired disease and affects the thoracolumbar spine. DAVF results from an abnormal anastomosis between a spinal radiculomeningeal artery and radicular vein. This anastomosis leads to venous perimedullary arterialization and venous congestion, reduced cord perfusion, and subsequent chronic cord ischemia. Spinal cord edema may occur distant to the site of DAVF and often progresses in the caudocranial orientation.

DAVF can be frequently confused with degenerative cervical or lumbar stenosis, diabetic neuropathy, and other disorders with similar symptoms that affect this age group. Imaging is paramount to quickly determine the correct diagnosis, which is important because affected patients with longer delays to diagnosis have been shown to improve the least following treatment (33).

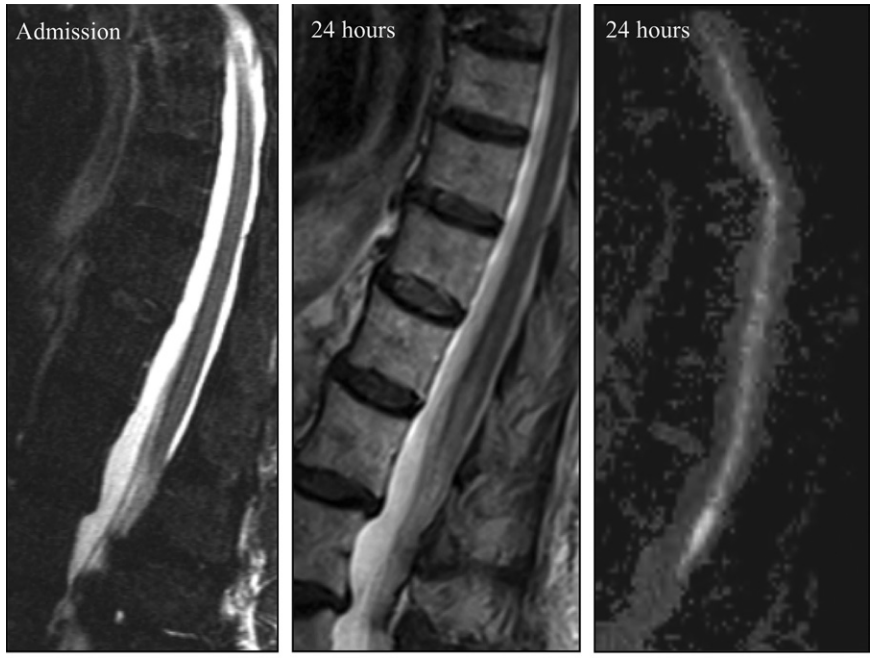

Figure 20. Spinal cord infarction in a 72-year-old man with a sudden onset of paraplegia and numbness. **(a)** Sagittal STIR image of the thoracic spine obtained at hospital admission shows normal spinal cord signal intensity. **(b)** Repeat sagittal STIR image obtained 24 hours later shows that a central abnormal T2-hyperintense intramedullary signal has developed. **(c)** Concurrent sagittal diffusion-weighted image shows diffuse intramedullary signal intensity, consistent with acute spinal cord infarction.

On MR images, the spinal cord typically is enlarged over multiple spinal levels and has central T2 hyperintensity with flame-shaped margins. A T2-hypointense rim may be seen and probably represents deoxygenated blood within the surrounding dilated capillary vessels. Of note, edema may not be present in cases of early DAVF detection. Multiple serpentine perimedullary flow voids from the arterialized and distended venous plexi often are seen and are key findings for a correct and prompt diagnosis. It is important to note that in cases of slow flow during early DAVF, these venous plexi may not be well seen at T2-weighted MRI. In such cases, contrast-enhanced MRI is the most reliable modality for visualizing dilated serpentine enhancing perimedullary vessels, which are suggestive of DAVF (Fig 21) (33). Ill-defined diffuse enhancement of the affected cord caused by the chronic breakdown of the blood–spinal cord barrier is often present. MR angiography and selective spinal digital subtraction angiography are useful for DAVF detection and catheter angiography guidance. DAVFs are treated with endovascular embolization, open surgical ligation, or a multimodality approach.

Inflammatory Causes

Multiple Sclerosis.—Multiple sclerosis (MS) is an autoimmune cell-mediated demyelinating disease that affects the brain and spinal cord, with lesions separated over time and space. It preferentially involves women, particularly those between the ages of 20 and 40 years. MS may be asymptomatic or manifest with paresthesias, muscle weakness, gait disturbance, bowel dysfunction, and/or bladder dysfunction. The CSF typically shows oligoclonal bands. MRI reveals focal discrete or ill-defined T2-hyperintense spinal cord lesions, with isolated spinal lesions seen in 10%–20% of cases. The cervical spine is most commonly affected. The lesions are often peripheral, with a preference for dorsal and lateral white matter tracts; oval or wedge shaped; and asymmetric (34).

Unlike with intramedullary tumors, with MS, there is no perilesional cord edema or marked cord expansion. Enhancing lesions represent acute to subacute demyelination, and the enhancement pattern changes with the evolution of inflammation, often from focal to ill-defined enhancement. It has been suggested that an incomplete ring enhancement pattern is specific for the diagnosis of MS (35). Cord atrophy may be seen during later stages of MS and correlates with clinical disability. MRI of the brain helps in determining the correct diagnosis, as abnormal white matter signal intensity in a periventricular, pericallosal, cerebellar, or brainstem distribution at T2-weighted imaging strongly suggests a diagnosis of MS (Fig 22).

Neuromyelitis Optica Spectrum Disorder.—Neuromyelitis optica (NMO) is an inflammatory disease of the central nervous system that typically reveals seropositivity for the astrocytic aquaporin-4 immunoglobulin G (AQP4-IgG) water channel receptor. The classic triad of NMO consists of optic neuritis, longitudinally extensive transverse myeli-

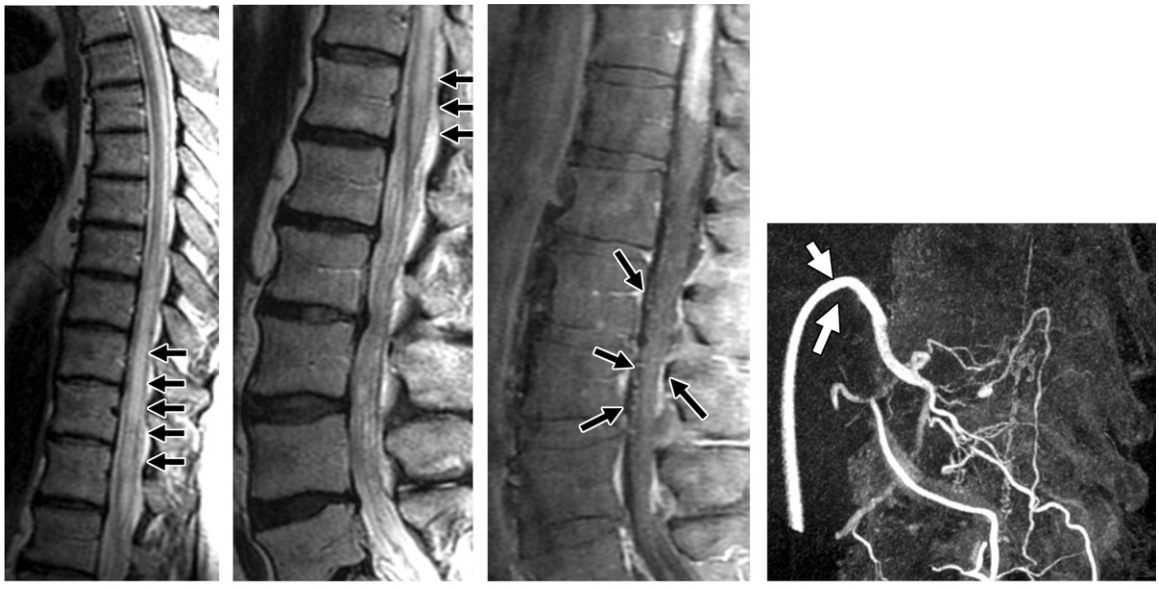

Figure 21. DAVF in a 63-year-old man who presented with bilateral leg numbness. **(a–c)** Sagittal T2-weighted **(a, b)** and contrast-enhanced T1-weighted **(c)** MR images of the thoracic and lumbar spine show an expanded and enhancing spinal cord from the T8 vertebral level to the conus medullaris, with central T2 hyperintensity, flame-shaped margins, and a T2-hypointense peripheral rim (arrows in **a** and **b**). There are multiple dilated intradural veins (arrows in **c**), which are best seen on contrast-enhanced images and appear as subtle flow voids on T2-weighted images. **(d)** MR angiogram of the thoracic spine shows dilated early-filling right T10 vertebral level perimedullary veins with a right T10 radiculomedullary feeding artery (arrows), consistent with DAVF. The incidental focal vascular dilatation medial to the fistula probably represents an aneurysm of the proximal aspect of the artery of Adamkiewicz. Although a fistula is present at the T10 level, the spinal cord involvement occurs in the caudocranial direction.

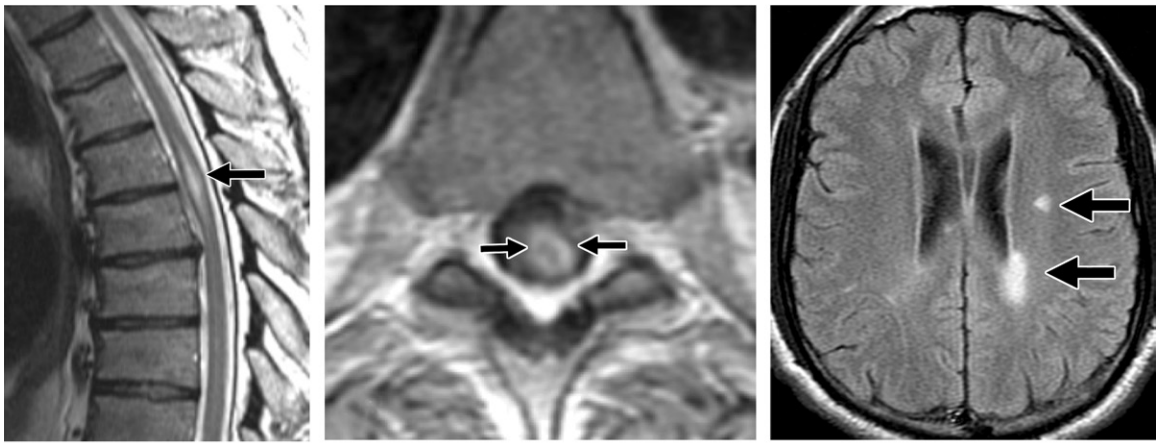

Figure 22. MRI findings in a 37-year-old man with a history of MS who presented with new-onset chest wall numbness. **(a, b)** Sagittal T2-weighted **(a)** and axial contrast-enhanced T1-weighted **(b)** MR images at the T5 vertebral level show a focal eccentric intramedullary T2-hyperintense lesion (arrows), with mild cord expansion and ring enhancement. **(c)** Axial fluid-attenuated inversion-recovery brain MR image shows T2-hyperintense periventricular foci (arrows), which are typical of demyelinating lesions.

tis involving more than three vertebral segments, and serologic analysis findings positive for AQP4-IgG antibody. The spectrum of NMO disorders includes AQP4-IgG–positive and AQP4-IgG–negative forms of NMO, as well as NMO disorders coexisting with other autoimmune diseases.

Similar to patients with MS, patients with NMO may have relapses. However, unlike with MS, with NMO there is no gradual decline in functional status between the relapses (36,37). Importantly, many medications used for the treatment of MS may cause NMO to worsen. A minority of patients with clinical characteristics of NMO and seronegativity for AQP4-IgG have a detectable serum myelin oligodendrocyte glycoprotein (MOG) antibody. Fewer than 20% of patients with NMO have oligoclonal bands at CSF analysis.

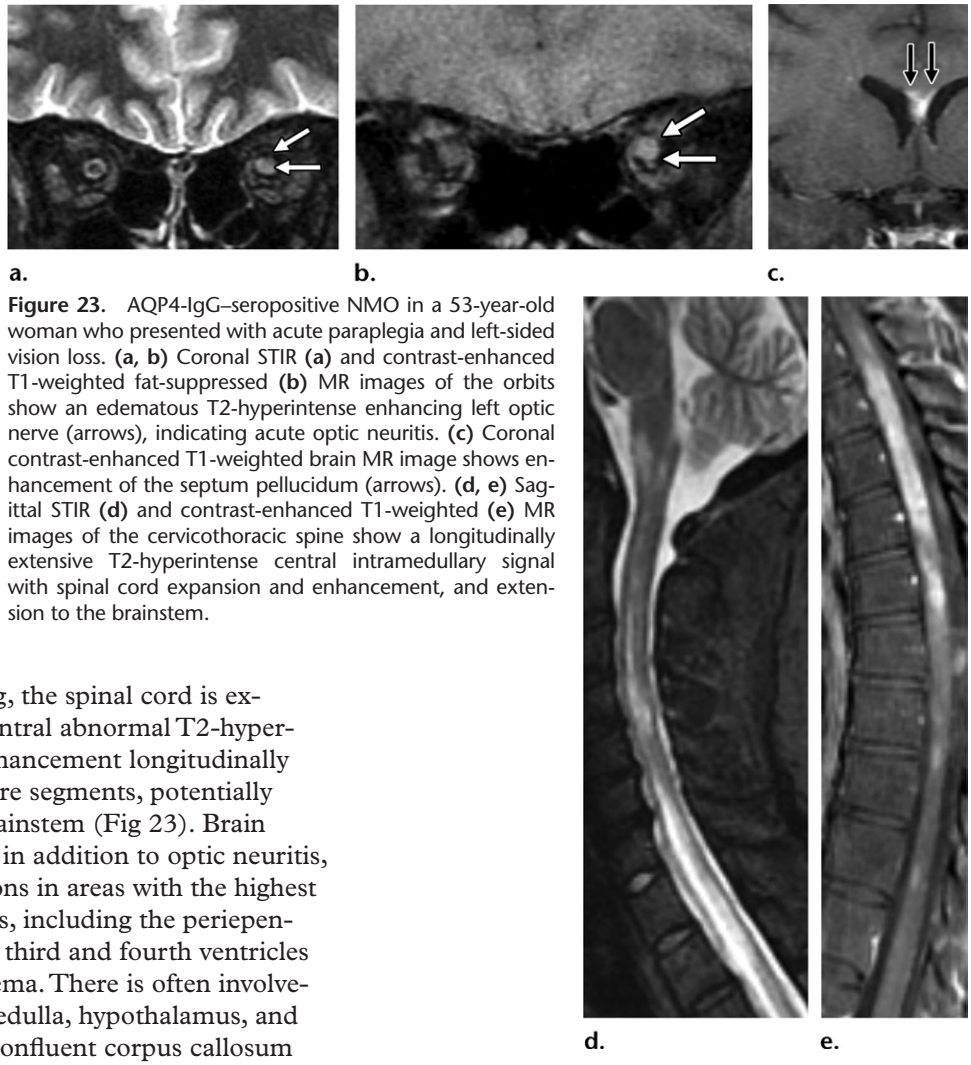

Figure 23. AQP4-IgG–seropositive NMO in a 53-year-old woman who presented with acute paraplegia and left-sided vision loss. **(a, b)** Coronal STIR **(a)** and contrast-enhanced T1-weighted fat-suppressed **(b)** MR images of the orbits show an edematous T2-hyperintense enhancing left optic nerve (arrows), indicating acute optic neuritis. **(c)** Coronal contrast-enhanced T1-weighted brain MR image shows enhancement of the septum pellucidum (arrows). **(d, e)** Sagittal STIR **(d)** and contrast-enhanced T1-weighted **(e)** MR images of the cervicothoracic spine show a longitudinally extensive T2-hyperintense central intramedullary signal with spinal cord expansion and enhancement, and extension to the brainstem.

In the acute setting, the spinal cord is expanded and shows central abnormal T2-hyperintense signal and enhancement longitudinally involving three or more segments, potentially extending into the brainstem (Fig 23). Brain MRI typically shows, in addition to optic neuritis, T2-hyperintense lesions in areas with the highest aquaporin-4 receptors, including the periependymal surfaces of the third and fourth ventricles and at the area postrema. There is often involvement of the dorsal medulla, hypothalamus, and thalamus, with long confluent corpus callosum lesions. Bright spotty lesions, described as T2-hyperintense foci with signal intensity similar to that of CSF within a T2-hyperintense spinal cord lesion, are suggestive of NMO (38).

Acute Disseminated Encephalomyelitis.—Acute disseminated encephalomyelitis (ADEM) is considered to represent a postinfectious or postvaccination sequela that involves widespread demyelination affecting the brain and spinal cord. Multiple viral and bacterial diseases have been implicated in the development of ADEM and include varicella, rubella, measles, Epstein-Barr virus, and mycoplasma infection. Although the exact mechanism of this condition is not well understood, it is suspected to be secondary to an autoimmune response to a myelin antigen (39).

ADEM typically affects children and young adults. The onset usually is rapid, with systemic symptoms including myalgia, headache, nausea, vomiting, drowsiness following a multifocal neurologic disorder with encephalopathy, cranial nerve palsy, ataxia, and paresis.

Spinal MRI reveals mild cord expansion with multifocal T2-hyperintense flame-shaped enhancing white matter lesions, which may be similar in appearance to MS lesions (31). The spinal involvement can be focal or segmental (Fig 24). Unlike polyphasic MS lesions, ADEM lesions are of the same age, indicating a monophasic disorder. Brain involvement is common and consists of patchy asymmetric T2-hyperintense regions involving the gray matter–white matter junction. The cranial nerves and gray matter, the basal ganglia and thalami in particular, can be involved; this is atypical with MS. Corpus callosum involvement is infrequent.

The CSF usually demonstrates lymphocytic pleocytosis, increased protein levels, and increased pressure. Oligoclonal bands are rare. ADEM responds to steroids, and recovery most frequently occurs within weeks or months, with complete recovery in 50% of cases (39).

Postviral Acute Transverse Myelitis.—Postviral acute transverse myelitis represents an acute inflammatory condition of the spinal cord. This disease occurs either secondary to a direct viral

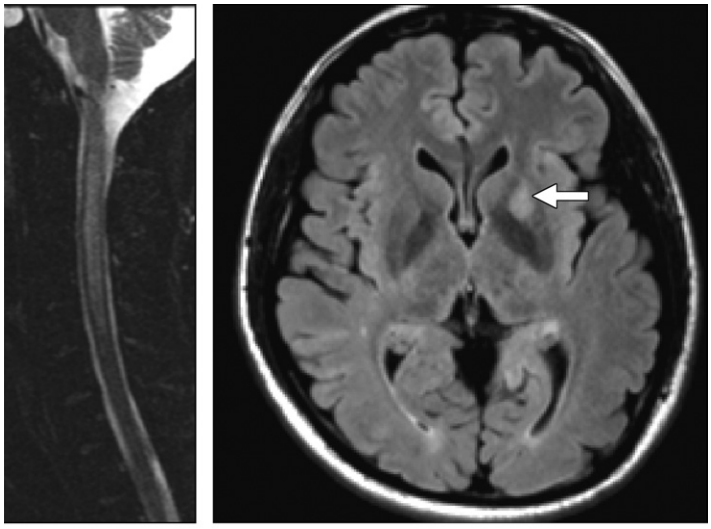

a. b.

Figure 24. ADEM in a 20-year-old man who initially presented with a decreased level of consciousness and lower extremity weakness. **(a)** Sagittal STIR MR image of the cervical spine shows mild cord expansion at the C2–C7 spinal level, with central longitudinally extensive intramedullary T2 hyperintensity. **(b)** Axial fluid-attenuated inversion-recovery MR image of the brain shows abnormal high T2 signal intensity in the left putamen (arrow), which is typical of the gray matter involvement in ADEM. These signal intensity abnormalities were resolved on MR images obtained 2 months later.

infection or as a postviral immune response. Enteroviruses are the most common pathogens, with signs of acute myelopathy developing after a febrile illness (40). On MR images, the spinal cord has an edematous appearance, with a segmental contiguous T2-hyperintense signal in the affected regions and variable patchy enhancement. At T1-weighted MRI, the spinal cord can have central low signal intensity, simulating syrinx, that is higher than the signal intensity of the CSF. The CSF demonstrates elevated mononuclear cells and protein levels. Brain involvement is not common.

Idiopathic Acute Transverse Myelitis.—Idiopathic acute transverse myelitis is the diagnosis of exclusion in the setting of bilateral rapid development of myelopathy. With this disease, there is a well-defined sensory level, evidence of inflammation at CSF analysis, and clinical symptom progression to nadir within 4 hours to 21 days (41). Radiologically, *idiopathic acute transverse myelitis* is defined as longitudinally extensive central intramedullary T2 hyperintensity involving gray and white matter, with expansion of the spinal cord, involvement of two or more vertebral levels, and variable contrast enhancement. Thus, in the absence of other definitive clues, acute transverse myelitis can be added to the differential diagnosis of most noncompressive myelopathies. For this reason, an initial diagnosis of idiopathic transverse myelitis is frequently discounted at additional workup. In prior studies (42), a more specific diagnosis, most commonly MS or spinal cord infarction, has been established in approximately 70% of cases initially diagnosed as idiopathic acute transverse myelitis.

Conclusion

The occurrence of acute myelopathy in a nontraumatic setting constitutes a medical emergency in which spinal MRI is frequently ordered as the first step in the patient's workup. Symptoms of myelopathy may have a compressive cause that can be further localized to the extradural, intradural extramedullary, or intramedullary compartments of the spinal canal. Use of a compartmental approach in combination with clinical and laboratory findings aids in refining the diagnosis and determining the appropriate surgical or nonsurgical management.

Noncompressive myelopathy represents abnormal intramedullary signal intensity without an underlying space-occupying lesion. It has a wide range of vascular, metabolic, inflammatory, infectious, and demyelinating causes with seemingly overlapping imaging appearances. The differential diagnosis may be refined by considering the location and longitudinal extent of the abnormal signal intensity within the cord, pertinent clinical history, and laboratory findings.

Acknowledgment.—The authors thank Dr. Zlatko Minev for creating the drawing in Figure 2.

Disclosures of Conflicts of Interest.—**B.K.** *Activities related to the present article:* disclosed no relevant relationships. *Activities not related to the present article:* received book royalties from Cambridge University Press. *Other activities:* disclosed no relevant relationships.

References

1. Parizel PM, van der Zijden T, Gaudino S, et al. Trauma of the spine and spinal cord: imaging strategies. Eur Spine J 2010;19(Suppl 1):S8–S17.
2. New PW, Cripps RA, Bonne Lee B. Global maps of nontraumatic spinal cord injury epidemiology: towards a living data repository. Spinal Cord 2014;52(2):97–109 [Published correction appears in Spinal Cord 2014;52(5):417.]
3. Fehlings MG, Vaccaro A, Wilson JR, et al. Early versus delayed decompression for traumatic cervical spinal cord injury: results of the Surgical Timing in Acute Spinal Cord Injury Study (STASCIS). PLoS One 2012;7(2):e32037.
4. Arce D, Sass P, Abul-Khoudoud H. Recognizing spinal cord emergencies. Am Fam Physician 2001;64(4):631–638.

5. Fraser S, Roberts L, Murphy E. Cauda equina syndrome: a literature review of its definition and clinical presentation. Arch Phys Med Rehabil 2009;90(11):1964–1968.
6. Sakka L, Gabrillargues J, Coll G. Anatomy of the Spinal Meninges. Oper Neurosurg (Hagerstown) 2016;12(2):168–188.
7. Bilsky MH, Laufer I, Fourney DR, et al. Reliability analysis of the epidural spinal cord compression scale. J Neurosurg Spine 2010;13(3):324–328.
8. Tetreault L, Goldstein CL, Arnold P, et al. Degenerative cervical myelopathy: A spectrum of related disorders affecting the aging spine. Neurosurgery 2015;77(Suppl 4):S51–S67.
9. Williams AL, Murtagh FR, Rothman SLG, Sze GK. Lumbar disc nomenclature: version 2.0. AJNR Am J Neuroradiol 2014;35(11):2029.
10. Mochida K, Komori H, Okawa A, Muneta T, Haro H, Shinomiya K. Regression of cervical disc herniation observed on magnetic resonance images. Spine 1998;23(9):990–995; discussion 996–997.
11. Song KJ, Kim KB, Lee KB. Sequestrated thoracic disc herniation mimicking a tumoral lesion in the spinal canal: a case report. Clin Imaging 2012;36(4):416–419.
12. McNamee J, Flynn P, O'Leary S, Love M, Kelly B. Imaging in cauda equina syndrome: a pictorial review. Ulster Med J 2013;82(2):100–108.
13. Kunam VK, Velayudhan V, Chaudhry ZA, Bobinski M, Smoker WRK, Reede DL. Incomplete Cord Syndromes: Clinical and Imaging Review. RadioGraphics 2018;38(4):1201–1222.
14. Shweikeh F, Saeed K, Bukavina L, Zyck S, Drazin D, Steinmetz MP. An institutional series and contemporary review of bacterial spinal epidural abscess: current status and future directions. Neurosurg Focus 2014;37(2):E9.
15. Guerado E, Cerván AM. Surgical treatment of spondylodiscitis: An update. Int Orthop 2012;36(2):413–420.
16. Yeom JA, Lee IS, Suh HB, Song YS, Song JW. Magnetic resonance imaging findings of early spondylodiscitis: Interpretive challenges and atypical findings. Korean J Radiol 2016;17(5):565–580.
17. Pierce JL, Donahue JH, Nacey NC, et al. Spinal Hematomas: What a Radiologist Needs to Know. RadioGraphics 2018;38(5):1516–1535.
18. Mak KS, Lee LK, Mak RH, et al. Incidence and treatment patterns in hospitalizations for malignant spinal cord compression in the United States, 1998-2006. Int J Radiat Oncol Biol Phys 2011;80(3):824–831.
19. Savage P, Sharkey R, Kua T, et al. Malignant spinal cord compression: NICE guidance, improvements and challenges. QJM 2014;107(4):277–282.
20. Cavaliere R, Schiff D. Epidural spinal cord compression. Curr Treat Options Neurol 2004;6(4):285–295.
21. Rizvi T, Wintermark M, Schiff D. Imaging of Epidural Spinal Cord Compression. In: Newton HB, ed. Handbook of Neuro-Oncology Neuroimaging. 2nd ed. London, England: Academic Presss/Elsevier, 2016.
22. Gibbs WN, Nael K, Doshi AH, Tanenbaum LN. Spine Oncology: Imaging and Intervention. Radiol Clin North Am 2019;57(2):377–395.
23. Sohawon D, Lau KK, Lau T, Bowden DK. Extra-medullary haematopoiesis: a pictorial review of its typical and atypical locations. J Med Imaging Radiat Oncol 2012;56(5):538–544.
24. Bartels RHMA, Brunner H, Hosman A, van Alfen N, Grotenhuis JA. The Pathogenesis of Ventral Idiopathic Herniation of the Spinal Cord: A Hypothesis Based on the Review of the Literature. Front Neurol 2017;8:476.
25. French H, Somasundaram A, Biggs M, et al. Idiopathic intradural dorsal thoracic arachnoid cysts: A case series and review of the literature. J Clin Neurosci 2017;40:147–152.
26. Agarwal N, Shah J, Hansberry DR, Mammis A, Sharer LR, Goldstein IM. Presentation of cauda equina syndrome due to an intradural extramedullary abscess: a case report. Spine J 2014;14(2):e1–e6.
27. Shim DM, Oh SK, Kim TK, Chae SU. Intradural extramedullary tuberculoma mimicking en plaque meningioma. Clin Orthop Surg 2010;2(4):260–263.
28. Ledbetter LN, Leever JD. Imaging of Intraspinal Tumors. Radiol Clin North Am 2019;57(2):341–357.
29. Jeon JH, Hwang HS, Jeong JH, Park SH, Moon JG, Kim CH. Spinal schwannoma: analysis of 40 cases. J Korean Neurosurg Soc 2008;43(3):135–138.
30. Küker W, Weller M, Klose U, Krapf H, Dichgans J, Nägele T. Diffusion-weighted MRI of spinal cord infarction: high resolution imaging and time course of diffusion abnormality. J Neurol 2004;251(7):818–824.
31. Sheerin F, Collison K, Quaghebeur G. Magnetic resonance imaging of acute intramedullary myelopathy: radiological differential diagnosis for the on-call radiologist. Clin Radiol 2009;64(1):84–94.
32. Weidauer S, Nichtweiss M, Lanfermann H, Zanella FE. Spinal cord infarction: MR imaging and clinical features in 16 cases. Neuroradiology 2002;44(10):851–857.
33. Fox S, Hnenny L, Ahmed U, Meguro K, Kelly ME. Spinal dural arteriovenous fistula: a case series and review of imaging findings. Spinal Cord Ser Cases 2017;3(1):17024.
34. Muccilli A, Seyman E, Oh J. Spinal Cord MRI in Multiple Sclerosis. Neurol Clin 2018;36(1):35–57.
35. Klawiter EC, Benzinger T, Roy A, Naismith RT, Parks BJ, Cross AH. Spinal cord ring enhancement in multiple sclerosis. Arch Neurol 2010;67(11):1395–1398.
36. Ciccarelli O, Cohen JA, Reingold SC, Weinshenker BG; International Conference on Spinal Cord Involvement and Imaging in Multiple Sclerosis and Neuromyelitis Optica Spectrum Disorders. Spinal cord involvement in multiple sclerosis and neuromyelitis optica spectrum disorders. Lancet Neurol 2019;18(2):185–197.
37. Tackley G, O'Brien F, Rocha J, et al. Neuromyelitis optica relapses: Race and rate, immunosuppression and impairment. Mult Scler Relat Disord 2016;7:21–25.
38. Hyun JW, Kim SH, Jeong IH, Lee SH, Kim HJ. Bright spotty lesions on the spinal cord: an additional MRI indicator of neuromyelitis optica spectrum disorder? J Neurol Neurosurg Psychiatry 2015;86(11):1280–1282.
39. Garg RK. Acute disseminated encephalomyelitis. Postgrad Med J 2003;79(927):11–17.
40. Cassidy H, Poelman R, Knoester M, Van Leer-Buter CC, Niesters HGM. Enterovirus D68: The New Polio? Front Microbiol 2018;9:2677.
41. Transverse Myelitis Consortium Working Group. Proposed diagnostic criteria and nosology of acute transverse myelitis. Neurology 2002;59(4):499–505.
42. Zalewski NL, Flanagan EP, Keegan BM. Evaluation of idiopathic transverse myelitis revealing specific myelopathy diagnoses. Neurology 2018;90(2):e96–e102.